Pergamon

SCIENCE DIRECT®

Bioorganic & Medicinal Chemistry Letters 13 (2003) 1463–1467

BIOORGANIC & MEDICINAL CHEMISTRY LETTERS

Design, Synthesis, and Structure–Activity Relationship of a New Class of Amidinophenylurea-Based Factor VIIa Inhibitors

Otmar Klingler,[a,*] Hans Matter,[a] Manfred Schudok,[a] S. Paul Bajaj,[b] Joerg Czech,[a] Martin Lorenz,[a] Hans Peter Nestler,[a] Herman Schreuder[a] and Peter Wildgoose[a]

[a]*Aventis Pharma Deutschland GmbH, Building G878, D-65926 Frankfurt, Germany*

[b]*Department of Pharmacological & Physiological Sciences and Internal Medicine, Saint Louis University Health Sciences Center, St. Louis, MI 63110, USA*

Received 5 November 2002; revised 23 December 2002; accepted 3 February 2003

Abstract—Selective inhibition of coagulation factor VIIa has recently gained attraction as interesting approach towards antithrombotic treatment. Using parallel synthesis supported by structure-based design and X-ray crystallography, we were able to identify a novel series of amidinophenylurea derivatives with remarkable affinity for factor VIIa. The most potent compound displays a K_i value of 23 nM for factor VIIa.

Activated factor VII (fVIIa) plays a pivotal role in the initiation of blood coagulation. Tissue factor (TF), a cofactor and allosteric regulator of fVIIa which is localized on the surface of subendothelial cells, is another important protein in the early steps of the coagulation cascade.[1–4] The fVIIa/TF complex efficiently hydrolyzes the zymogen coagulation factors (fX, fIX and fVII) to the corresponding active serine protease forms, culminating in the conversion of prothrombin to thrombin which eventually transforms fibrinogen to fibrin in the final stage of clotting.[5,6]

The pathophysiological role of an excessively active coagulation cascade and subsequent inappropriate thrombus formation in blood vessels has been well recognized. Currently available anticoagulants show undesirable properties and side effects, like bleeding, that limit their usefulness in the treatment of thrombotic disorders and encourage efforts to discover new low molecular weight compounds which inhibit the enzymes of the blood coagulation cascade.[7,8] Several reports point out that inhibiting the early blood coagulation stages cause significantly fewer bleeding events.[9] Therefore, the fVIIa/TF complex is seen as promising target for developing novel therapeutic anticoagulants.[10–17] In this publication, we describe the identification and structure activity relationship studies of a novel series of amidinophenylurea derivatives as potent inhibitors of the fVIIa/TF complex.[18]

The initial representatives of the amidinophenylurea series, compounds **1** and **2**, were discovered from focused screening of serine protease directed compounds from our internal collection.[19] The selection of the screening set was guided by the identification of relevant protein–ligand interactions from the public X-ray structure of the fVIIa/TF complex with a covalent inhibitor (1DAN).[20]

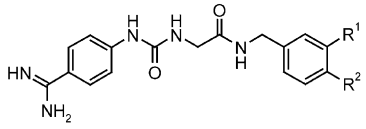

cpds	R^1	R^2	fVIIa K_i [μM]
1	Cl	H	2.17
2	H	$-N(CH_3)_2$	1.94

Figure 1. Chemical structures of initial amidinophenylureas.

Consistent manual and automated docking results based on this structure plus structural experience from other serine proteases led us to postulate that the benzamidine is situated in the fVIIa catalytic domain S1 pocket, interacting with the carboxylate side chain of Asp189 at the bottom of this pocket, the Oγ atom of Ser190 and to the carbonyl oxygen of Gly219 by

*Corresponding author. Tel.: +49-69-305-83313; fax: +49-69-305-21618; e-mail: otmar.klingler@aventis.com

0960-894X/03/$ - see front matter © 2003 Elsevier Science Ltd. All rights reserved.
doi:10.1016/S0960-894X(03)00168-9

additional hydrogen bonds.[21–24] Those studies also led to the hypothesis that both urea NH protons interact with the active triad residue Ser195. The second aromatic ring was postulated to occupy the more hydrophobic, shallow binding site area bridging the S2 and S4 pockets above the Trp215-Gly216 beta-sheet region. This binding site hypothesis prompted for a rational design using the amidinophenylurea scaffold as privileged template for exploring the both the S2 and S4 pockets.

Compounds **1**–**19**, **21**, and **24**–**27** were readily prepared according to methods outlined in Scheme 1. Reaction of aminobenzonitrile derivatives with various isocyanates in DMF yielded nitrile intermediates **3**. Of the different procedures for amidine formation utilized, the two step Pinner reaction proved to be the most convenient method.[25] Thus, intermediates **3** were sequentially treated with HCl/ethanol and NH_3/ethanol to afford the benzamidines **4**, which were converted to the key intermediates **5**. The final step in the synthesis sequence was partly carried out by automated parallel synthesis coupling the acids **5** (TOTU/DMF)[26] with amino building blocks H_2N-R^4. Protection of the amidino groups was not necessary. The amino building blocks were commercially available or prepared from ketone precursors by reductive amination.

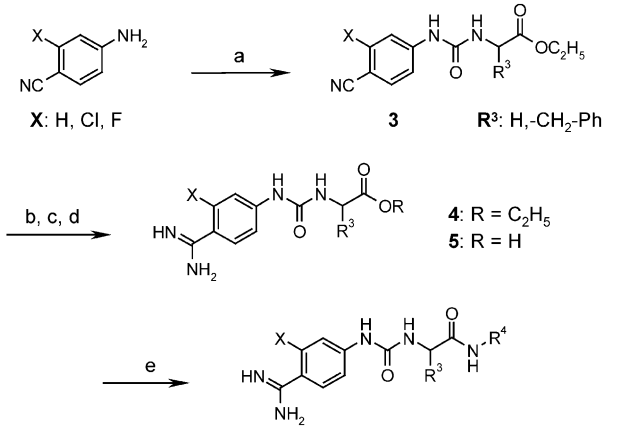

Scheme 1. Synthesis of compounds **1**–**19**, **21**, **24**–**27**. Reagents and conditions: (a) ethoxycarbonyl-CHR^3 isocyanate, DMF; (b) HCl, EtOH; (c) NH_3, EtOH; (d) NaOH, H_2O; (e) H_2N-R^4, TOTU, DMF, *N*-ethylmorpholine.

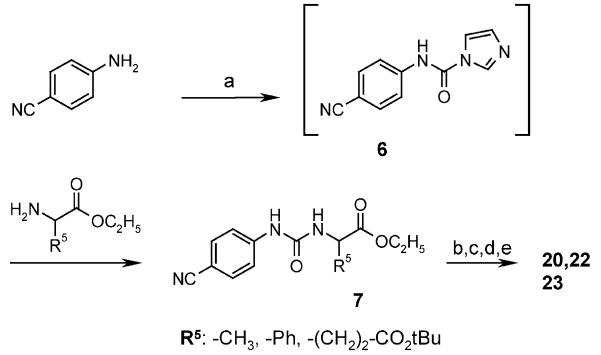

Scheme 2. Synthesis of compounds **20**, **22** and **23**. Reagents and conditions: (a) carbonyldiimidazole, DMF, 80 °C; (b) HCl, EtOH; (c) NH_3, EtOH; (d) NaOH, H_2O; (e) H_2N-R^4, TOTU, DMF, *N*-ethylmorpholine.

Table 1. In vitro activity for compounds **8**–**19**

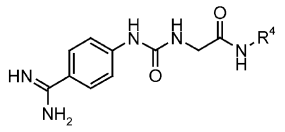

Compd	R^4	K_i (μM) fVIIa	fXa	Thrombin
8	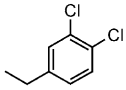	0.97	14.5	10.1
9	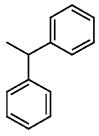	0.73	nd	nd
10	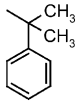	7.62	> 10	> 50
11	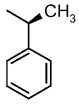	0.43	> 10	50.7
12	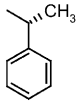	20.2	> 10	> 50
13	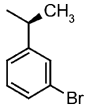	0.027	> 10	15.9
14	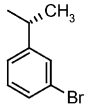	31.0	nd	nd
15	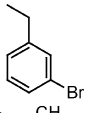	1.51	7.8	> 50
16	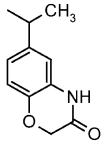	0.023	> 10	16.4
17	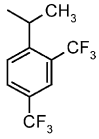	0.027	> 10	> 100
18	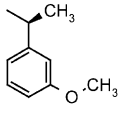	0.035	> 10	18.2
19	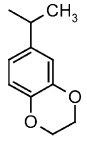	0.067	> 10	11.2

nd: Not determined.

For synthesis of compounds **20**, **22** and **23**, an alternative route depicted in Scheme 2 proved more efficient. Reaction of aminobenzonitrile with carbonyldiimidazole at 80 °C provided the intermediate **6** in situ, which was converted to the urea building blocks **7** by addition of amino acid derivatives. The final reaction steps were conducted as described in Scheme 1.

Initial variations of the R^4 phenyl group did not significantly improve fVIIa affinity (Fig. 1, **1**, **2**, Table 1, **8**, **15**). Subsequently, a branching point was introduced at the α-position of the R^4 substituent. Incorporation of a second phenyl ring yielded in compound **9** with enhanced affinity ($K_i = 0.73$ μM).

For compound **9** we solved its complex with human fVIIa/TF by X-ray structure analysis at 2.2 Å (Fig. 2), thus validating our initial model about favorable protein–ligand interactions for biological affinity.[27] In addition to the expected amidinophenyl binding to S1, one urea NH interacts directly with the active triad

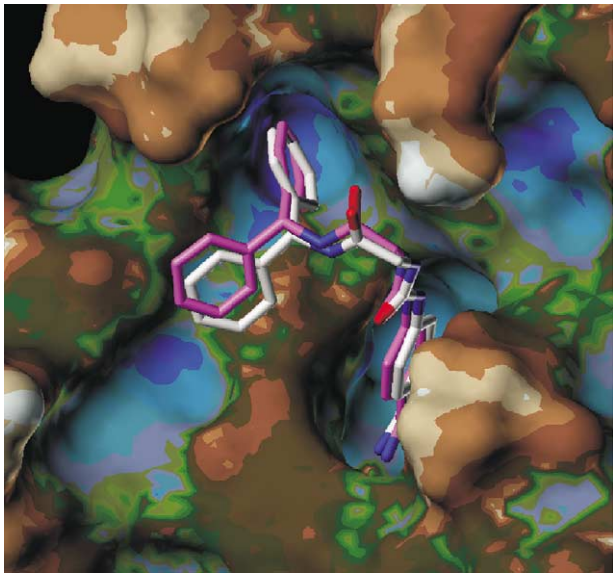

Figure 2a. Comparison of X-ray structure (white carbon atoms) to proposed binding mode (magenta) for compound **9** in factor VIIa. The protein is displayed with a MOLCAD surface indicating local curvature. The conformational model for **9** was generated using flexible docking with QXP.

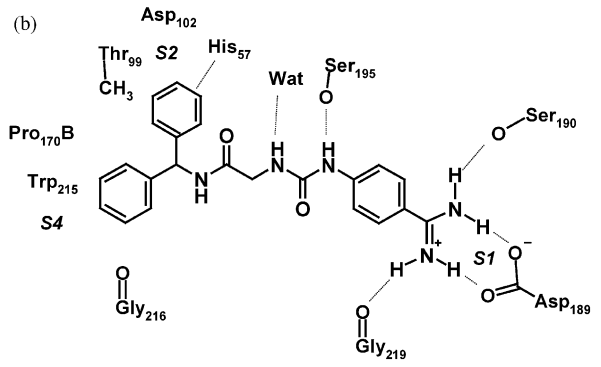

Figure 2b. Schematic interactions of **9** with key residues of human factor VIIa.

Ser195-Oγ (3.1 Å), the other via a structurally conserved water moleule (3.2 Å). Especially remarkable were the interactions of one distal phenyl ring with the protease S2 pocket. This ring is stacked on top of the imidazole ring from the active triad His57 (~3.3 Å), its *para*-carbon atom is in close distance to the active triad Asp102 carboxylate (3.2 Å) and the hydrophobic portion of Thr99 (3.5 Å to Cα), which itself separates S2 from the open S4 pocket. The other phenyl ring is situated ~3.5 Å on top of the Gly216 carbonyl oxygen in the hydrophobic binding site area next to S4.

The replacement of the S2 directed phenyl substituent by a smaller, hydrophobic methyl group led to a significant increase in binding affinity (**11**, $K_i = 0.43$ μM). This was supported by modeling studies, suggesting an improved complementarity of hydrophobic protein–ligand interactions in this area, if the remaining phenyl ring comes closer to the protein surface region. Therefore our further optimization was based on the X-ray crystal structure of compound **9**. In contrast, introduction of a second methyl group in α-position of compound **10** resulted in a decreased affinity. Among the mono-α-methyl substituted derivatives, compounds **13** and **16**–**18** exhibited particularly high biological activity ($K_i = 0.023$–0.035 μM). The most active fVIIa inhibitors were found to be highly selective against related proteases like factor Xa and thrombin, as summarized in Table 1. Several enantiomeric pairs of *R*/*S* analogues were prepared to investigate the stereochemical orientation of the methyl group at the α-position of R^4. For example, the *S*-phenyl(methyl) analogue **11** is 50-fold more potent than its *R*-phenyl(methyl) counterpart **12**, and *S*-3-bromophenyl(methyl) inhibitor **13** is 1150-fold more potent than its *R*-3-bromophenyl-(methyl) enantiomer **14**. This suggests in accord with our binding site model the importance of filling the S2 pocket with small hydrophobic substituents.

To determine how variations at the central unit of the urea scaffold would affect activity, the glycyl moiety was replaced by several amino acids, as shown in Table 2. Incorporation of alanine generated compound **20** which is about 50-fold less potent than the corresponding glycine derivate **8** (Table 1). Compound **21** with phenylalanine moiety is 10-fold less potent than glycine derivative **2**. Affinity is also decreased by a phenylglycine at the central core. The glycine derivative **13** (Table 1) is 120-fold more potent than the phenylglycine analogue **23**. Glutamic acid derivative **22** was the most active compound within this series, but also showed a 20-fold decrease in potency relative to compound **13**. Thus, within this series the glycyl residue proved to be the most preferred residue at this position. Obviously, none of the introduced substituents led to favorable interactions to fVIIa, as both Gly Cα protons are directed towards the solvent exposed area of the binding site.

Finally, our interest was to discern electronic effects of a substituent in the benzamidine core moiety, as a lower basicity of this fragment is generally accepted to produce a more favorable oral bioavailability.[29] Hence,

Table 2. In vitro activity for compounds **20–23**

Compd	Structure	K_i (μM) fVIIa
20	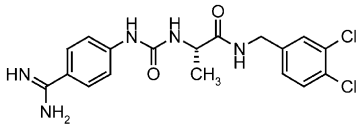	45.8
21	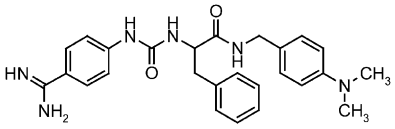	20.9
22	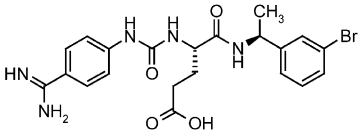	0.54
23	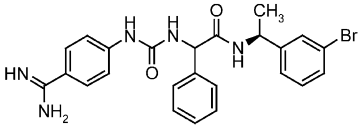	3.2

halogen atoms were introduced into the *ortho*-position to the amidino group, resulting in compounds **24–27**. The modifications, which included incorporation of a chlorine, afforded analogues **24** and **26** with 140-fold and 60-fold loss of activity relative to the parent derivatives **13** and **19**. The effect of a fluorine substituent is less marked. However, compounds **25** and **27** are 4-fold and 7-fold less active than the unsubstituted analogues **13** and **16**. According to modeling studies, this reduced biological affinity by substitution in the S1 pocket was attributed to unfavorable steric interactions between one amidinophenyl NH_2 group and the *ortho*-halogen atoms, as compared to the less bulky hydrogen. Obviously, the favorable dihedral angle of $\sim 30°$ for the amidine plane relative to the phenyl ring could not be maintained in these derivatives. As expected, the experimental p*K*a values decrease from 11.2 to 11.3 of compounds **13**, **16** and **19** to 10.7 to 10.9 of compounds **24**, **25**, **26** and **27** (Table 3).[28]

Table 3. In vitro activity for compounds **24–27**

Compd	Structure	K_i (μM) fVIIa
24	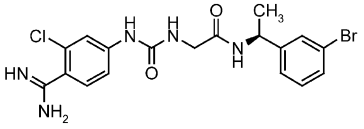	3.76
25	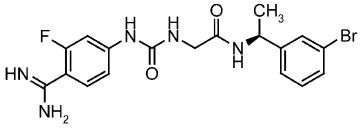	0.12
26	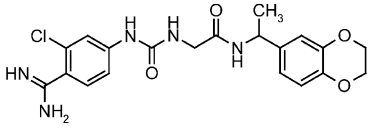	3.94
27	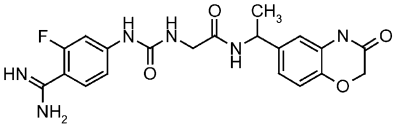	0.47

In summary, we have described the SAR of a series of factor VIIa inhibitors with various modifications around an amidinophenylurea template. The incorporation of branched amines attached to the core template led to a significant improvement of biological activity and high selectivity against related proteases. The best compounds (**13** and **16–18**) have K_i values between 23 and 35 nM against fVIIa without significant inhibition of factor Xa or thrombin. Hence, this series constitutes a promising area for further studies supported by structure-based design.

Acknowledgements

The authors would like to thank Peter Below, Silke Herok, Iris Hessler, Alexander Liesum and Andrea Struppmann for their technical assistance.

References and Notes

1. Kirchhofer, D.; Banner, D. W. *Trends in Cardiovascular Medicine* **1997**, *7*, 316.
2. Petersen, L. C.; Hedner, U.; Wildgoose, P. In *Mol. Basis Thromb. Hemostasis,* High, K. A., Roberts, H. R., Eds., Dekker, New York, 1995, pp 147–165.
3. Gallagher, K. P.; Mertz, T. E.; Chi, L.; Rubin, J. R.; Uprichard, A. C. G. *Handbook of Experimental Pharmacology* **1999**, *132*, 421.
4. Morrisey, J. H. *Thromb. Haemostasis* **2001**, *86*, 66.
5. Kirchhofer, D.; Nemerson, Y. *Curr. Opin. Biotechnol.* **1996**, *7*, 386.
6. Eigenbrot, C.; Kirchhofer, D. *Trends in Cardiovascular Medicine* **2002**, *12*, 19.
7. Hirsh, J.; Weitz, J. I. *Lancet* **1999**, *353*, 1431.
8. Adang, A. E. P.; Rewinkel, J. B. M. *Drugs Future* **2000**, *25*, 369.
9. Girard, T. J.; Nicholson, N. S. *Curr. Opin. Pharmacol.* **2001**, *1*, 159.
10. Young, W. B.; Kolesnikov, A.; Rai, R.; Sprengeler, P. A.; Leahy, E. M.; Shrader, W. D.; Sangalang, J.; Burgess-Henry, J.; Spencer, J.; Elrod, K.; Cregar, L. *Bioorg. Med. Chem. Lett.* **2001**, *11*, 2253.
11. Jakobsen, P.; Horneman, A. M.; Persson, E. *Bioorg. Med. Chem.* **2000**, *8*, 2803.
12. Jakobsen, P.; Ritsmar Petersen, B.; Persson, E. *Bioorg. Med. Chem.* **2000**, *8*, 2095.
13. Kohrt, J. T.; Filipski, K. J.; Rapundalo, S. T.; Cody, W. L.; Edmunds, J. J. *Tetrahedron Lett.* **2000**, *41*, 6041.
14. Roussel, P.; Bradley, M.; Kane, P.; Bailey, C.; Arnold, R.; Cross, A. *Tetrahedron* **1999**, *55*, 6219.
15. Aliagas-Martin, I.; Artis, D.R.; Dina, M. S.; Flygare, J. A.; Goldsmith, R. A.; Munroe, R. A.; Olivero, A. G.; Pastor, R.; Rawson, T. E.; Robarge, K. D.; Sutherlin, D. P.;

Weese, K. J.; Zhou, Z.; Zhu, Y. PCT Patent WO 0041531. *Chem. Abstr*. **2000**, *133*, 101383.
16. Senokuchi, K.; Ogawa, K. PCT Patent WO 9941231. *Chem. Abstr*. **1999**, *131*, 184864.
17. Ackermann, J.; Alig, L.; Chucholowski, A.; Groebke, K.; Hilpert, K.; Kuehne, H.; Obst, U.; Weber, L.; Wessel, H. P. PCT Patent WO 0035858. *Chem. Abstr*. **2000**, *133*, 59090.
18. Klingler, O.; Schudok, M.; Nestler, H. P.; Matter, H.; Schreuder, H. EP Patent 1162194. *Chem. Abstr*. **2001**, *136*, 19952.
19. Inhibitory activity expressed as inhibition constant Ki toward fVIIa/tissue factor was determined using a chromogenic assay as described in: Ostrem, J. A.; Al-Obeidi, F.; Safar, P.; Safarova, A.; Stringer, S. K.; Patek, M.; Cross, M. T.; Spoonamore, J. C.; LoCascio, J. C.; Kasireddy, P.; Thorpe, D. S.; Sepetov, N.; Lebl, M.; Wildgoose, P.; Strop, P. *Biochemistry* **1998**, *37*, 1053.
20. Banner, D.; D'Arcy, A.; Chene, C.; Winkler, F. K.; Guha, A.; Konigsberg, W. H.; Nemerson, Y.; Kirchhofer, D. *Nature* **1996**, *380*, 41.
21. Rarey, M.; Kramer, B.; Lengauer, T.; Klebe, G. *J. Mol. Biol*. **1996**, *261*, 470.
22. McMartin, C.; Bohacek, R. S. *J. Comp. Aided Mol. Des* **1997**, *11*, 333.
23. Heiden, W.; Goetze, T.; Brickmann, J. *J. Comp. Chem*. **1993**, *14*, 246.
24. Modeling was done using Sybyl 6.5-6.8 (Tripos). Energy calculations were based on the MMFF94s force field (Halgren, T. *J. Comp. Chem*. **1999**, *20*, 720–729.). Protein-ligand complexes were minimized using the quasi-Newton-Raphson procedure. For manual docking, ligands were placed in the fVIIa binding site and optimized treating all side chains within 4 Å flexible. Automated docking was carried out using FlexX (21) and QXP (22).
25. (a) Pinner, A.; Klein, F. *Chem. Ber*. **1878**, *11*, 1825. (b) Gautier, J. A.; Miocque, M.; Farnoux, C. C. In *The Chemistry of Amidines and Imidates*; Patai, S., Ed.; Wiley: New York, 1975; pp 283–348.
26. TOTU: *O*-[Ethoxycarbonyl)cyanomethylenamino]-*N*,*N*,*N*′,*N*′-tetramethyl-uronium tetrafluoro-borate; König, W.; Breipohl, G.; Pokorny, P.; Birkner, M. *Proceedings of the 21st European Peptide Symposium 1990*; Giralt, E., Andren, D, Eds.; ESCOM, Leiden, 1990, p 143.
27. The factor VIIa-tissue factor complex was crystallized in hanging drops at pH 6.5 using conditions described by Kirchhofer, D.; Guha, A.; Nemerson, Y.; Konigsberg, W. H.; Vilbois, F.; Chène, C.; Banner, D.; D'Arcy, A. *Prot. Struct. Func. Gen*. **1995**, *22*, 419. Data were collected at beam-line ID 14-3 of the European Synchrotron Radiation Facility (ESRF) in Grenoble. The data were processed with MOSFLM: Leslie, A.G.W.; Powell, H.R. *NATO Science Series, Series I: Life and Behavioural Sciences* **2001**, *325*, 61. The crystal diffracted to 2.2 Å with an overall Rsym of 5.7%. The space group was $P2_12_12_1$ with a = 70.08 Å, b = 81.74 Å and c = 126.17 Å. Initial phases were calculated using the structure by Banner (20) as starting model. The inhibitor was fitted using Quanta and refined using CNX (Accelrys). The final R-factor was 20.0% (R-free = 25.0%). The benzamidine and urea parts of the inhibitor are well defined in the electron density maps, while the two phenyl groups and the peptide linker have poor electron density indicating some disorder.
28. The p*K*a values were measured by UV difference spectroscopy on a Sirius SGA profiler.
29. Linusson, A.; Gottfries, J.; Olsson, T.; Örnskov, E.; Folestad, S.; Nordén, B.; Wold, S. *J. Med. Chem*. **2001**, *44*, 3424.